Coordination Chemistry Reviews 354 (2018) 121–134

Contents lists available at ScienceDirect

Coordination Chemistry Reviews

journal homepage: www.elsevier.com/locate/ccr

Review

Reaction-based BODIPY probes for selective bio-imaging

Safacan Kolemen [a,*,1], Engin U. Akkaya [a,b,*]

[a] UNAM-Institute of Material Science and Nanotechnology, Bilkent University, Ankara 06800, Turkey
[b] Department of Chemistry, Bilkent University, Ankara 06800, Turkey

ARTICLE INFO

Article history:
Received 9 May 2017
Received in revised form 22 June 2017
Accepted 24 June 2017
Available online 17 July 2017

Keywords:
Chemodosimeters
BODIPY
Bio-thiols
Reactive oxygen/nitrogen species
Gaseous molecules
Fluorescence imaging
Live cell imaging

ABSTRACT

Complex intracellular environment of cells, which involves interaction of a large variety of bio-molecules, is a dynamic medium with full of important information that can be recovered as well as many unanswered questions. It is highly critical to image and track biologically relevant molecules in their native media without interfering with the regular cellular processes in order to gather as much data as possible to illuminate intricacies of the biological mechanisms. To that end, small-molecule fluorescent probes have been extensively developed during the last few decades with the help of current advances in imaging technologies. Although conventional probes utilizing non-covalent supramolecular interactions with the analyte of interest are successful, significant effort has been also put into the design of reaction-based probes (chemodosimeters). Chemodosimeters exploit selective reactions of analytes with fluorophores in attempt to improve the selectivity of the probes, address the limitations of former sensors and broaden the palette of useful probes. Various types of fluorophore scaffolds can be used in the design of chemodosimeters for visualization of different analytes. In this review, we highlight the 4,4-difluoro-4-bora-3a,4a-diaza-s-indacene (BODIPY) based chemodosimeters which have been used to image bio-thiols, reactive oxygen/nitrogen species, and gaseous molecules in living cells.

Contents

* Corresponding authors at: UNAM-Institute of Material Science and Nanotechnology, Bilkent University, Ankara 06800, Turkey.
E-mail addresses: safacan@bilkent.edu.tr (S. Kolemen), eua@fen.bilkent.edu.tr (E.U. Akkaya).
[1] Current address: Koc University, Department of Chemistry, Rumelifeneri Yolu, 34450 Sariyer, Istanbul, Turkey.

http://dx.doi.org/10.1016/j.ccr.2017.06.021
0010-8545/

1. Introduction

Cytoplasm of the cells contains myriad of ions, small molecules, and bio-molecules that are continuously interacting with each other in a dynamic environment [1]. These complex and time-dependent interactions are vital for all living organisms and they are tightly regulated by the cells. However, any mismanagement in this regard can cause critical malfunctions and generally triggers the formation of various disease states. Consequently, it is highly important to track ongoing cellular processes at molecular-level in living cells in order to understand and clarify the biological roles and significance of these intracellular players. To that end, fluorescence imaging is a promising candidate to visualize living cells in their native environment, because it offers spatial and temporal resolution, high selectivity and sensitivity as well as real-time, fast, easy, and inexpensive imaging techniques thanks to a large variety of available probe (fluorophore) scaffolds and recent developments in fluorescence and confocal microscopy instrumentation.

2. Reaction-based fluorescent probes

Fluorescent molecular probe development has evolved into an attractive field of study particularly after Tsien's pioneering study on fluorescent Ca^{2+} detection in 1980 [2], followed by a large number of reports emerging at a steady pace with worldwide participation [3–8]. The common strategy, especially in the case of earlier examples is to use reversible and non-covalent supramolecular interactions in the design of fluorescent probes [9–15]. Accordingly, most of the synthetic fluorescent probes contain a binding site and a signaling core, which are linked or integrated to each other with a rapid communication in-between. The selective interaction of a probe with a target analyte through a binding site yields measurable optical changes in the signaling core (in the form of emission intensity or emission wavelength), which can be detected with various simple spectroscopic techniques.

The major requirement for fluorescent probe design is to ensure the high selectivity and affinity toward the analyte of interest in a complex intracellular medium, where many different types of reactions are taking place. In order to improve the selectivity of molecular probes in such a dynamic environment, it is highly rational to exploit different reactivities of target analytes. To that end, "reaction-based probes", also known as "chemodosimeters" have been employed extensively in bio-imaging studies during the last decade. In a reaction-based approach, the observable signal results from an analyte-specific bio-orthogonal reaction that is mostly irreversible. A typical chemodosimeter consists of a fluorophore core as a signaling unit that is modified with a functional group, which serves as a specific reaction site for the analyte. As in the case of a conventional supramolecular approach, the fluorescence response can either be modulated by OFF-ON/ON-OFF manner, or ratiometrically [16]. In the former case, the probe is either virtually non-fluorescent unless an analyte-specific reaction takes place and reveals its fluorescence, or it is initially emissive and a reaction quenches the fluorescence. On the other hand, ratiometric design results in an emission wavelength shift following the reaction between species of interest and the probes. An efficient reaction-based probe should have: (i) a high selectivity in the presence of competing species that may have similar reactivities, (ii) a less tendency to interfere with endogenous processes taking place in the cellular environment, (iii) enough product stability to yield an optical signal change [1].

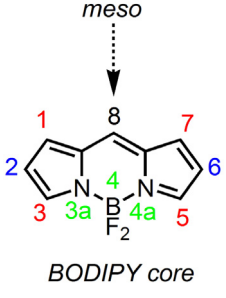

Fig. 1. Molecular structure of a BODIPY core.

3. BODIPY-based chemodosimeters

The choice of a signaling unit while designing a reaction-based probe is highly critical to harvest the best optical performance from the probe. Among potential fluorophore scaffolds BODIPY (4,4-difluoro-4-bora-3a,4a-diaza-s-indacene) (Fig. 1) dye has attracted great attention as a fluorescent module and has been widely applied in bio-imaging applications because of its high absorption coefficient, high fluorescence quantum yield, relatively sharp absorption and emission spectra, photostability, easy functionalization, and neutral net charge [16,17]. Current advances in BODIPY chemistry also allow the synthesis of red-shifted BODIPYs [18]. Far-red and near-IR probes have advantages in the development of small molecule fluorescent probes for biological applications since absorption and emission in long-wavelength region generate low autofluorescence, minimal phototoxicity, and negligible background from biomolecules [18]. Furthermore, red-shifted probes can also be suitable for *in vivo* imaging, which is highly useful for practical applications due to deeper tissue penetration of the incoming and outgoing light. The major drawback of BODIPY derivatives is their high hydrophobicity leading to low water solubility. However, this problem can be simply addressed by decorating the core structure with hydrophilic moieties through well-established examples of BODIPY chemistry. There are several excellent reviews on literature regarding the chemistry and spectroscopic properties of BODIPYs as well as some others highlighting BODIPY-based fluorescent probes [16–20]. This review, however, focuses on only the reaction-based BODIPY probes, which have been used to detect biological thiols, reactive oxygen/nitrogen species, and gaseous molecules in living cells. For further reading about reaction-based probes, readers may refer to previously published reviews on the literature [1,16,21,22].

3.1. Selective detection of bio-thiols

Biological thiols, namely cysteine (Cys), homocysteine (Hcy) and glutathione (GSH) are vital molecules for cells due to their important roles in maintaining redox homeostasis in biological systems [23,24]. These low molecular weight thiols are also known to be significant biomarkers for several acute and chronic diseases [24]. High Cys concentration, for instance, is clearly associated with myocardial and cerebral infractions, whereas Cys deficiency can induce liver damage, muscle and fat loss, skin lesions, growth problems in children, and cancer [25]. Moreover, Cys plays crucial roles in oxidation/reduction reactions of mitochondria related electron transport, as it is the main thiol source for iron-sulfur clusters. On the other hand, elevated level of Hcy has been linked to several vascular and renal disorders as well as Alzheimer's diseases [26]. Moreover, change in total plasma concentration of Hcy can be the risk factor for birth abnormalities and cognitive impairment in elder people [23]. Intracellular concentrations of Cys and Hcy are at micromolar levels; however, plasma concentration can reach up to a millimolar level (0.25–0.38 mM) [23]. GSH is the most abundant intracellular bio-thiol, which is the tri-peptide of cysteine, glycine,

and glutamic acid [27]. GSH is an effective antioxidant that undertakes important roles in controlling intracellular redox activities and signal transduction. It particularly appears in the oxidative stress control mechanism to maintain the redox homeostasis [23,24]. Abnormal level of cellular GSH is directly related to cardiovascular diseases, aging, and cancer, such that, its intracellular concentration is 2–50-fold higher in cancer cells compared to normal cells [28]. Considering their biological importance, it is highly critical to detect, monitor, and quantify each of these bio-thiols selectively under physiological conditions. To that end, fluorescence imaging has been extensively applied using BODIPY derivatives, which is one of the favorite fluorophore cores among possible scaffolds. Current fluorescence detection strategies of bio-thiols mostly utilize the strong nucleophilic character of thiols, directing researchers to design selective chemodosimeters. Typical reactions that have been used in conjugation with BODIPY dyes are: Michael addition, cyclization with aldehydes, cleavage of sulfonamide/sulfonate esters, and thiol-halogen substitution.

Michael addition type chemodosimeters have been extensively applied as thiol selective fluorescent probes due to the strong nucleophilicity of thiols [1,23,24]. Akkaya group designed two BODIPY based probes **1** and **2** both carrying a nitroalkene group, which acts as a Michael acceptor [29]. In both designs, gallic acid derived units were incorporated in order to improve the water solubility of the probes (Fig. 2). Compound **1** has an absorption maximum at 525 nm, while probe **2** has red-shifted absorption (623 nm) because of the extended π-conjugation. Nucleophilic attack of bio-thiols to the nitroalkene breaks the conjugation and stops intramolecular charge transfer (ICT), which causes a blue shift in the absorption spectra. Addition reaction also alters the excited state dynamics of the probes and blocks the photo-induced electron transfer (PeT) that takes place from electron rich trimethoxyphenyl moiety to the electron poor BODIPY core. Consequently, both probes show similar chromogenic and fluorescence turn-on responses to all bio-thiols in HEPES buffer:CH_3CN (80:20 v/v), however, the response to Cys is much faster than Hcy and GSH. Thus, by just controlling the reaction kinetics, exquisite selectivity for Cys was obtained.

In another work from Akkaya group [30], selective detection of GSH, which is known to be a challenging goal, was aimed. A BODIPY core bearing nitroalkene group was used again to satisfy the selective thiol reaction (compound **3**). However, in the design of **3**, aza-crown moiety was added to the *meso* position of BODIPY as an additional recognition side for the N-terminal ammonium group of GSH (Fig. 3). The probe is non-fluorescent ($\phi_F < 0.01$) due to the PeT taking place from aza-crown to BODIPY core. All of the three bio-thiols (Cys, Hcy and GSH) react with the nitroalkene rapidly at pH 6.0 buffer (mimicking the tumor tissue pH) as expected, yielding a slight blue-shift in absorption spectra, however, structural fit of the protonated N-terminal ammonium of GSH to aza-crown receptor is much better, resulting in more efficient disruption of PeT, and consequently, higher emission turn-on response with GSH compared to Cys/Hcy. The probe was also employed to monitor GSH distribution in human breast adenocarcinoma cells (MCF-7). As an additional experiment, HUVEC cells were treated with buthionine sulfoximine (BSO), a well-known inhibitor of γ-glutamylcysteine synthetase. Significant fluorescence decrease was observed in HUVEC cells upon BSO inhibition, further proving the selectivity of **3** toward GSH.

Cyclization reactions between aldehydes and thiols are among the widely used strategies for fluorescent sensing of Cys and Hcy. Molecular probes containing aldehyde functional groups can participate in 6- or 5-membered ring formation with suitable 1,3- or 1,2-aminothiols to form thiazolidines and thiazinanes, which results in dramatic changes in the optical properties of probes. However, GSH with its bulkier molecular structure is not suitable for a similar ring formation. Accordingly, Ravikanth et al. introduced a 3,5-bis(acrylaldehyde)-BODIPY **4** for selective detection of Cys and Hcy over GSH in living cells [31]. Reaction between the amine group of Cys/Hcy with α,β-unsaturated aldehyde, first forms an imine intermediate, which was followed by ring formation (Fig. 4). Upon Cys and Hcy titration, a blue shift was reported in absorption spectra and a remarkable turn-on at 567 nm was detected when the probe was excited at 510 nm. No fluorescence response was observed when the probe was treated with GSH

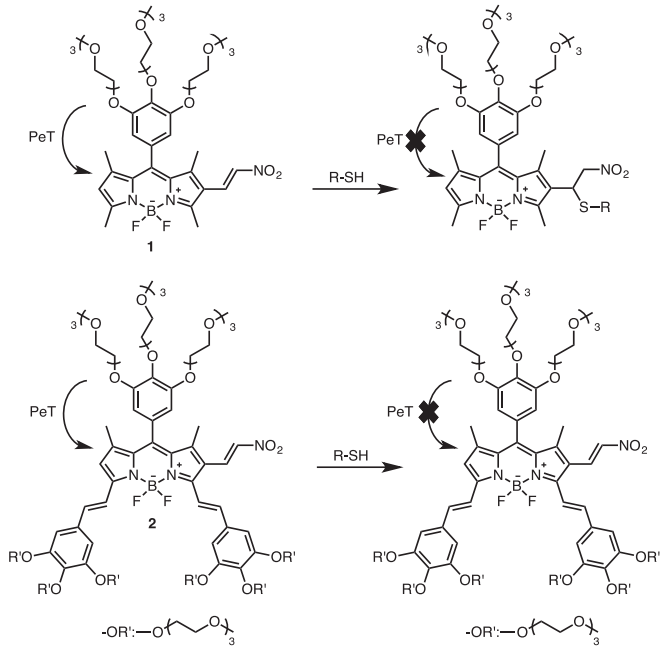

Fig. 2. Michael addition-based detection of bio-thiols.

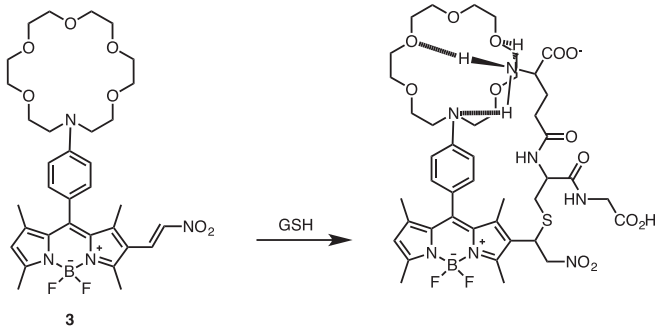

Fig. 3. Selective GSH detection with two recognition sites.

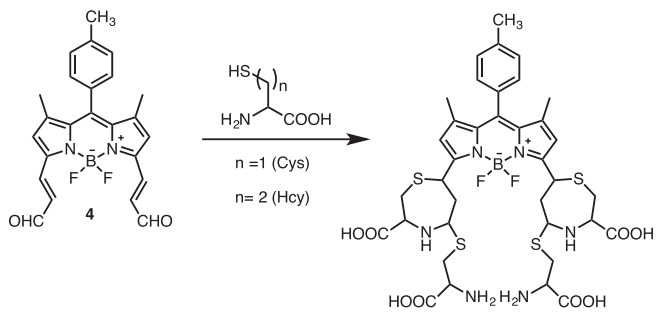

Fig. 4. Selective aldehyde cyclization reaction on a BODIPY core for imaging of Cys and Hcy in living cells.

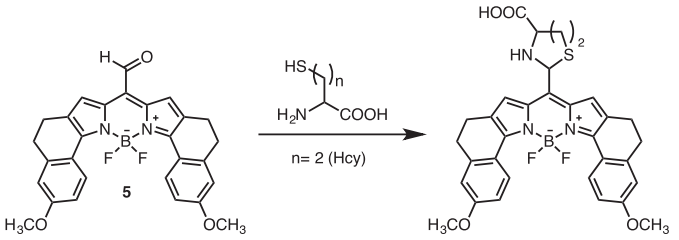

Fig. 5. Selective detection of HCY with a *meso*-formyl substituted BODIPY **5**.

and other competing amino acids. Compound **4** is also used to image the intracellular Cys/Hcy in HepG2 cells successfully.

Discrimination between Cys and Hcy is difficult due to their similar structures and reactivities. Consequently, reports introducing the selective detection of Hcy over Cys are limited in literature. To address this issue, Zhao and coworkers devised a NIR-emitting *meso*-aldehyde substituted BODIPY **5** [32]. While designing the probe, 1 and 7 positions were kept substituent-free in order to eliminate steric hindrance and enable the attack of thiols to aldehyde (Fig. 5). Probe **5** takes advantage of aldehyde cyclization reaction in order to realize the selective detection of Hcy. The probe is almost non-emissive ($\phi_F = 0.06$) in CH_3CN-water solution prior to Cys/Hcy addition. After treating the probe with Cys/Hcy in the same aqueous solution, absorption maximum was blue-shifted and a 30-fold turn-on ($\phi_F = 0.92$) response was reported in emission with Hcy. Reaction of the probe with Cys only causes 9-fold turn-on ($\phi_F = 0.39$) in fluorescence signal at 678 nm. Detailed kinetic measurements reveal that the probe reacts faster with Hcy to Cys, yielding potential selectivity toward Hcy based on reaction kinetics.

Thiol-halogen exchange reaction offers an alternative pathway for the detection of bio-thiols, specifically for GSH. This approach is highly promising since there are only few reports on selective GSH monitoring in literature, and discrimination of GSH from other bio-thiols is still a challenge. Yang et al. reported a pioneering example of thiol-halogen nucleophilic substitution approach for selective fluorescent sensing of GSH (Fig. 6) [33]. Chlorine on the chlorinated-BODIPY derivative **6** undergoes nucleophilic aromatic

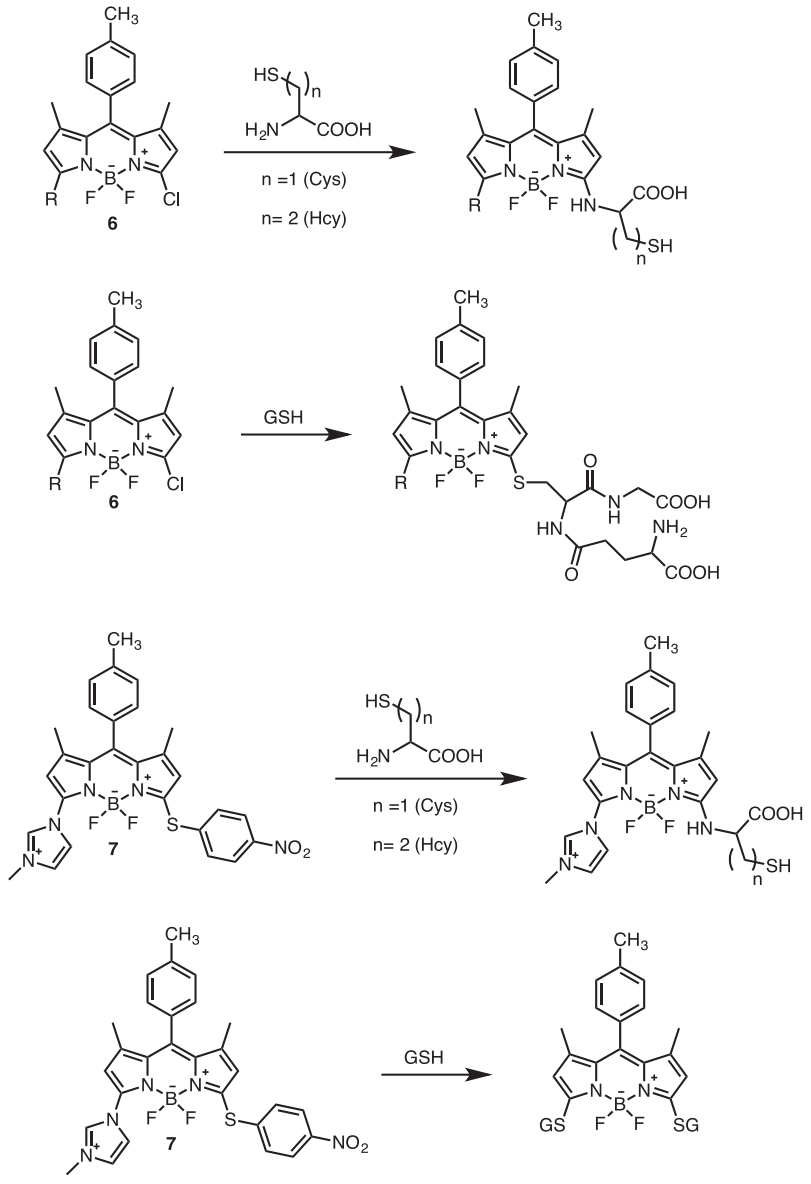

Fig. 6. Thiol-halogen exchange reactions on halogenated BODIPYs for the detection of GSH.

substitution with the thiolates of the bio-thiols. Although thioether adduct that was formed by GSH is stable, Cys/Hcy encounters further intramolecular replacement of thiolates with primary amine groups on Cys/Hcy, which involves the formation of 5- or 6-membered rings in the transition state. At the end, two products were obtained: the first one is the sulfur-substituted BODIPY (in the case of GSH), and the second one is amino-substituted BODIPY derivative (in the case of Cys/Hcy). As expected, these two products have different optical characteristics such that the absorption and emission maxima of amino-BODIPYs were blue shifted (λ_{ems} = 556 nm), whereas sulfur-BODIPY has red shifted absorption and emission spectra (λ_{ems} = 588 nm). Therefore, by monitoring the emission signal at 588 nm, the highly selective GSH probe was introduced, which was also applied to monitor intracellular GSH in HeLa cells. Yang group in their recent study further improved their initial design by improving the reactivity of the probe toward GSH (Fig. 6) [34]. Probe **7** contains an electron-withdrawing imidazolium group to increase the rate of nucleophilic aromatic substitution and improve the water solubility of the probe. Nitrothiophenol was also incorporated at on the BODIPY core both as a good leaving group for thiol triggered S_NAr reaction and a PeT acceptor, which makes the probe almost non-fluorescent and eliminates the background signal to a larger extent. Reaction of the nitrothiophenol moiety with Hcy/Cys forms amino-BODIPYs (λ_{ems} = 530 nm), as in the case of **6**, through substitution-rearrangement reaction, however, GSH reacts with both nitrothiophenol and imidazolium groups to yield disulfur-BODIPY with different photophysical properties (λ_{ems} = 588 nm). Again, by just controlling the excitation wavelength, discrimination between GSH and Cys/Hcy was satisfied. Compound **7** was also incubated with HeLa cells to perform dual color imaging of Cys and GSH. A remarkable fluorescence intensity increase was observed both in green (Cys) and red emissions (GSH), showing the applicability of the probe to live cell imaging.

Another exchange reaction was developed by Ahn et al. to monitor intracellular Cys (Fig. 7) [35]. The ratiometric probe **8** involves methylthio substituent at the *meso* position of BODIPY, which exchanges with biothiols Cys/Hcy to form thiol adducts. Further intramolecular substitutions yield amino-BODIPYs. Resulting BODIPYs have blue-shifted absorption and emission maxima (λ_{abs} = 400 nm, λ_{ems} = 467 nm) compared to the free probe and the thiol adduct that was formed by GSH. When the same concentrations of Cys and Hcy were used, the ratiometric response of **8** is comparable, however the probe was selectively responded to Cys under physiological concentrations because of the higher cellular concentration of Cys. The probe was also successfully employed to image Cys in zebra fish. Confocal images showed that eye and gill of zebra fish have a higher level of Cys compared to other organs.

Cleavage of sulfonamides and sulfonate esters are two well known reactions, which have been widely applied in reaction-based probe designs for selective detection of Cys/Hcy over GSH. James and coworkers introduced an elegant example of this approach by designing a red-emitting fluorescent resonance energy transfer (FRET) based probe **9** (Fig. 8) [36]. In their design, a simple BODIPY core, bearing a polyether chain was used as a FRET energy donor (λ_{abs} = 498 nm λ_{ems} = 511 nm), while monostyryl BODIPY with a 2,4-dinitrobenzenesulfonyl (DNBS) moiety acts as a FRET energy acceptor (λ_{abs} = 568 nm λ_{ems} = 586 nm). Although FRET is ON, the emission of acceptor cannot be observed due to the oxidative PeT caused by electron withdrawing DNBS group. Cleavage of DNBS moiety upon a reaction with Cys/Hcy forms 4-hydroxyphenyl and blocks PeT, which re-activates the red emission of the acceptor at 590 nm. Compound **9** is highly selective to Cys/Hcy over GSH and other amino acids. It was also demonstrated that the probe is capable of imaging cellular thiols in SGC-H446.

One of the important challenges of fluorescent probe design is to target specific organelles in order to satisfy the detection of bio-thiols localized in subcellular compartments. This challenging goal requires careful molecular design, which should involve both thiol specific reaction sites as well as specific targeting moieties. To that end, Talukdar et al. introduced a lysosome localized probe **10** for selective imaging of bio-thiols (Fig. 9) [37]. DNBS was used as a thiol reaction side and morpholine was employed to achieve lysosomal targeting. Compound **10** is almost non-fluorescent due to

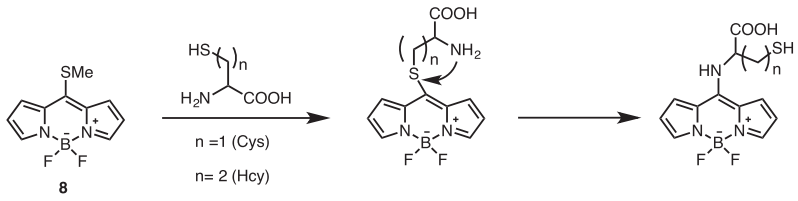

Fig. 7. Reactions taking place on **8** for imaging of Cys and Hcy.

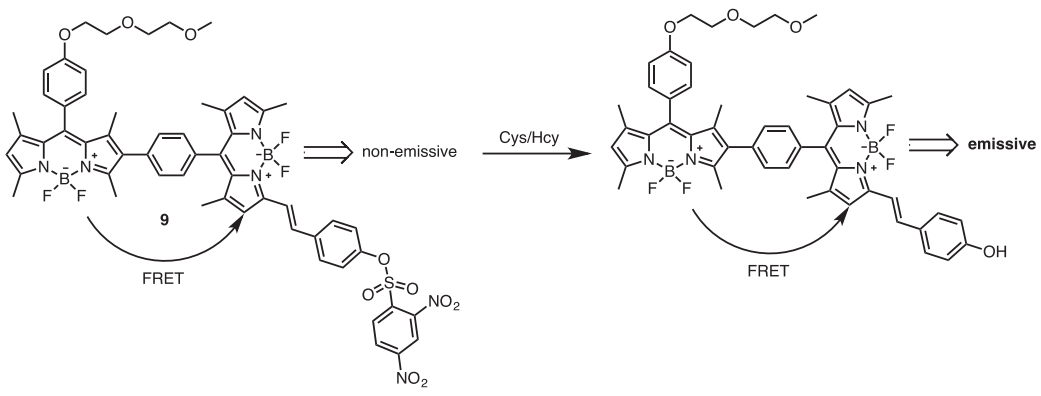

Fig. 8. Cleavage of sulfonate ester with Cys/Hcy yields an emissive product.

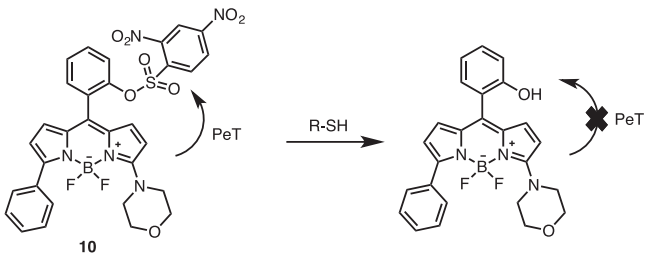

Fig. 9. A lysosome targeted BODIPY based probe for the detection of bio-thiols.

the DNBS induced PeT. Release of DNBS by bio-thiols resulted in an increased emission intensity. Co-localization experiments with green-emitting lysosome specific LysoSensor Green probe prove the localization of **10** in lysosomes and red emission from the probe demonstrates the potential of the probe to detect bio-thiols in living cells.

Recently, Zhao and coworkers described a mitochondria-targeting GSH sensitive probe **11** [38]. The probe utilizes a *para*-dinitrophenoxybenzyl pyridinium group at the *meso* position of a BODIPY derivative (Fig. 10). This group behaves as a sacrificial caging group, and upon reacting with bio-thiols, yields a pyridinium-BODIPY. Compound **11** is non-emissive because of PeT that was induced by 2,4-dinitro-phenoxyphenyl moiety. When bio-thiols are added, they react with dinitrophenyl group and release the sacrificial dinitrophenoxybenzyl module. The free pyridinium group also serves as a mitochondria-targeting group. It was observed that GSH reacts faster with the probe compared to Cys/Hcy and gives the highest turn-on response (32-fold) in the case of GSH. The unique behavior of GSH was attributed to its perfect structural fit with both cationic pyridinium moiety (which interacts electrostatically with the carboxylate end of bio-thiols) and thiol-reactive dinitrophenoxy group. Cys/Hcy also interact with the cationic pyridinium moiety, but they are away from the thiol reaction site because of their shorter chain. Confocal images of HeLa cells, which were incubated with **11**, display the intracellular GSH distribution in living cells and prove the mitochondria localization (checked by Mito-Tracker Green co-localization) of the probe.

3.2. Selective probes for ROS/RNS

Reactive oxygen species (ROS), including hydrogen peroxide (H_2O_2), hydroxyl radicals (·OH), hypochlorous acid/hypochlorite ions (HOCl/$^-$OCl), superoxide ($O_2^{\cdot-}$), and singlet oxygen ($^1O_2$), are produced extensively in aerobic organisms [39,40]. Although the major source of ROS formation is the mitochondrial respiration, they can be also generated upon UV light and infectious agents exposure [39]. ROS are highly critical for both physiological and pathological processes. These extremely unstable molecules play variety of roles in signaling pathways and they are needed for redox homeostasis and regular cell function. However, overproduction or any mismanagement of the ROS can induce oxidative stress, which may trigger the cellular aging and serious diseases such as cancer, neurodegeneration, diabetes, and cardiovascular complications [41]. At molecular level, they mostly cause the oxidation of lipids and proteins as well as mutations on DNA, which results in cell death.

Nitrogen-based analogs of ROS are known as reactive nitrogen species (RNS), which include nitric oxide (NO), peroxynitrite ($ONOO^-$), nitrogen dioxide (NO_2), and nitroxyl (HNO). These species are also involved in important biological processes such as signal transduction, neurotransmission, immune system control, and blood pressure modulation [42]. RNS are involved in oxidative reactions within the cells, thus, misregulation of RNS is highly associated with cancer, neurodegeneration, and inflammation [43]. Because of the aforementioned roles and the importance of ROS/RNS, they have been at the focus of particular interest during the last decade [43–46], which resulted in excellent fluorescent probes aiming to monitor intracellular ROS/RNS selectively and uncover their biological roles.

3.2.1. Detection of superoxide in living cells

Superoxide ($O_2^{\cdot-}$) is a very important ROS that is produced mostly through NADPH oxidase activity and electron transport mechanisms. It has a very short lifetime, which aggravates its detection in living cells [43]. There are several probes for selective detection of superoxide that employ different fluorophores [43]. Churchill et al. introduced a BODIPY based fluorescent probe bearing a diselenide moiety that links two BODIPY cores **12** (Fig. 11) [47]. It was highlighted that $O_2^{\cdot-}$ induced oxidation of selenium increases the emission intensity of the probe, which is otherwise almost non-fluorescent. The probe was also tested with several other ROS including HOCl, ·OH, H_2O_2, ^{t}BuOOH and ^{t}BuO· and no, or low turn-on responses were observed, indicating the selectivity of **12** toward superoxide. The addition of bio-thiols regenerates the parent probe and quenches the emission intensity. This reversible behavior, in principle, makes it possible to monitor dynamic superoxide fluxes in living cells. For further demonstration of applicability of the probe in living cells, it was incubated with MCF-7/ADR (breast cancer cell line). Cells were co-incubated with PMA

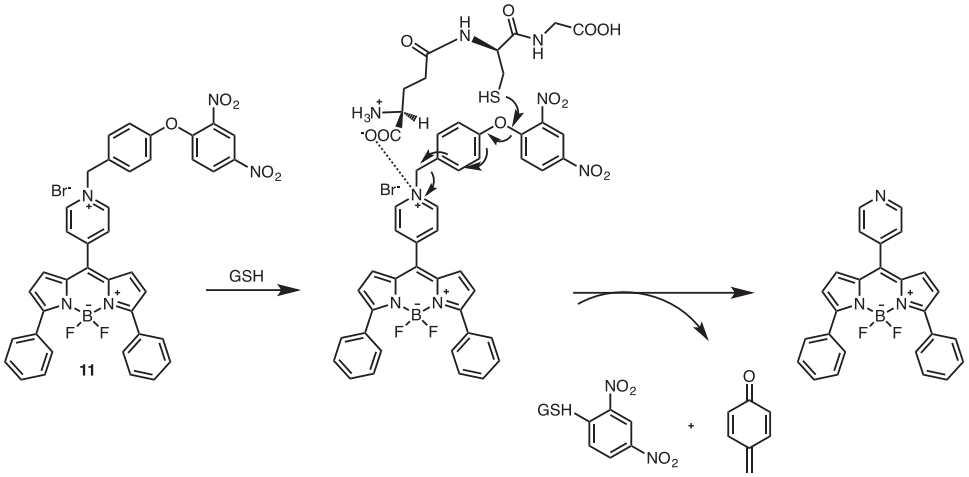

Fig. 10. A mitochondria targeted GSH selective BODIPY based probe **11**.

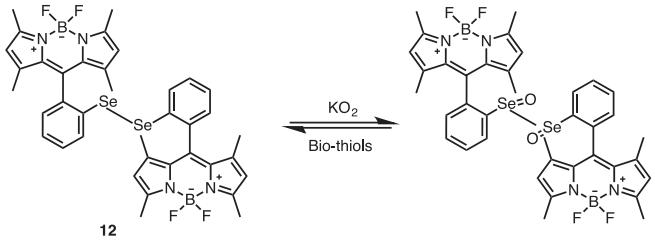

Fig. 11. Selenium oxidation-induced superoxide detection in living cells.

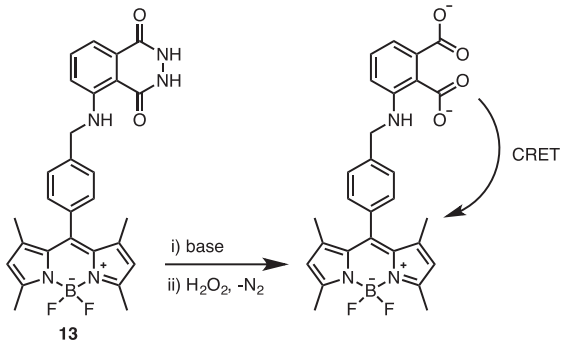

Fig. 12. A CRET based probe for superoxide imaging.

(phorbol-12-myristate 13-acetate) to overproduce superoxide within the cells. Confocal images display remarkable turn-on responses, suggesting selective intracellular detection of superoxide.

Rochford and co-workers described a chemiluminescent resonance energy transfer (CRET) cassette based on a BODIPY-luminol conjugate **13** in order to image intracellular superoxide [48]. The phenyl group at the *meso* position blocks electronic communication between the energy donor luminol and the acceptor BODIPY, while increasing the CRET efficiency (Fig. 12). Addition of H_2O_2 along with $CuSO_4$ in pH 10.0 buffer activates luminol chemiluminescence, which is followed by CRET and the detection of BODIPY emission. It was noted that luminol luminescence was also observed because of spectral mismatch and the CRET efficiency was found to be 64%. Cellular superoxide monitoring was also achieved in PMA-activated splenocytes, which were incubated with CRET cassette.

3.2.2. Detection of hypochlorous acid in living cells

Hypochlorous acid (HOCl) is another example of ROS, which is synthesized from hydrogen peroxide in the presence of myeloperoxidase (MPO) enzyme that acts as a catalyst. Abnormal levels of MPO and consequent change in HOCl concentration are associated with neurodegenerative and cardiovascular diseases as well as osteoarthritis [43]. Yang et al. used the strong oxidizing capacity of HOCl and designed a BODIPY based fluorescent probe carrying a *p*-methoxyphenol group at the *meso* position **14** (Fig. 13) [49]. The probe fluorescence was modulated by PeT mechanism and it

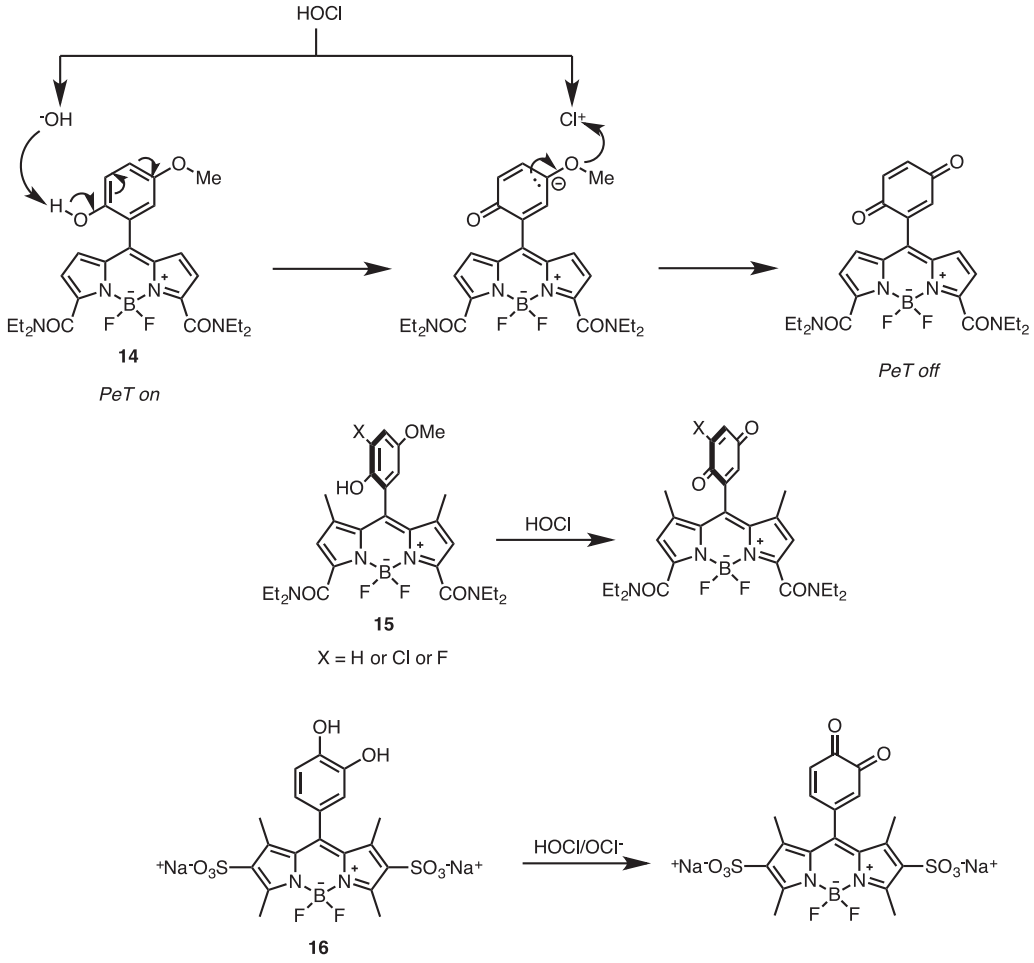

Fig. 13. Molecular structures of HOCl-selective probes and the detection mechanism.

is non-emissive prior to oxidation. The addition of NaOCl rapidly yields benzoquinone and blocks PeT. As a result, dramatic increase in emission intensity was detected. Fluorescence enhancement was not observed in the presence of other ROS/RNS, indicating the selectivity of the probe toward HOCl. Compound **14** is also able to image intracellular hypochlorous acid in RAW264.7 macrophages upon stimulation. The major drawback of **14** is epoxidation of the quinone moiety, which weakens fluorescence. To overcome this problem, Yang group introduced methyl groups on 1- and 7-positions of the BODIPY core **15** in order to restrict the rotation of *meso*-phenyl, which increases the fluorescence quantum yield of the oxidized product (Fig. 13) [50]. Another important modification is the *ortho*-substituted halogens (Cl, F) to prevent further oxidation of quinone group. In this way, a series of highly selective and chemostable probes were introduced. Incubating the probe with RAW264.7 cells and THP-1 human macrophages allows monitoring of cellular HOCl using confocal microscopy. In another report, Kim et al. developed a water-soluble analog (**16**) that contains *meso*-catechol unit as a selective reaction site for OCl^- (Fig. 13) [51]. Sulfonate groups at the 2- and 6-positions provide water solubility. The detection mechanism is similar and involves the oxidation of catechol to quinone in the presence of NaOCl in phosphate buffer, which results in emission intensity increase.

Wu and coworkers developed a highly selective HOCl probe **17** bearing an organoselenium group at the *meso* position of the BODIPY core (Fig. 14) [52]. The probe is non-emissive because of the PeT from selenium moiety to the electron acceptor BODIPY core. HOCl-induced oxidation of selenium blocks PeT and results in a highly emissive probe (λ_{ems} = 526 nm). Other ROS/RNS do not show any detectable fluorescence enhancement, confirming the selectivity of the probe. Compound **17** was also used to image intracellular HOCl in RAW264.7 cells successfully.

Intracellular HOCl and H_2S levels have great impact on neurodegeneration, specifically in Alzheimer's diseases. It was reported that H_2S levels decrease in Alzheimer patients, while neuronal HOCl production increases. Therefore, simultaneous monitoring of HOCl and H_2S is highly valuable. Han group reported a reversible probe **18** to image the redox cycle between HOCl and H_2S in living cells (Fig. 15) [53]. Selective oxidation of selenium re-activates the fluorescence as in the case of **17**. Following reduction of selenoxide to selenide quenches the fluorescence by turning-on the PeT mechanism. Fluorescence enhancement was detected only with HOCl in the presence of other competing ROS/RNS. On the other hand, fluorescent turn-off response is selective to H_2S among other intracellular reductants. Confocal images display selective imaging of both HOCl and H_2S in RAW264.7 cells upon stimulation. In another study [54], Han et al. also introduced a ratiometric fluorescent probe **19** for monitoring HBrO/H_2S redox cycle by employing a similar approach to **18**. The probe was modified with 4-methyoxylphenylselenide at 3- and 5-positions of the BODIPY core (Fig. 15). The addition of HBrO causes a blue shift in the absorption maximum, while 230-fold turn-on response was detected in the emission spectrum. Also compound **19** allows the monitoring of the redox cycle between HBrO/H_2S in RAW264.7 cells selectively.

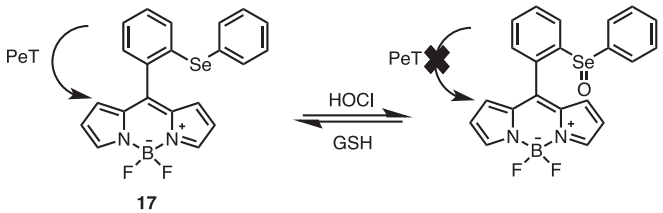

Fig. 14. Selenium oxidation for the detection of HOCl.

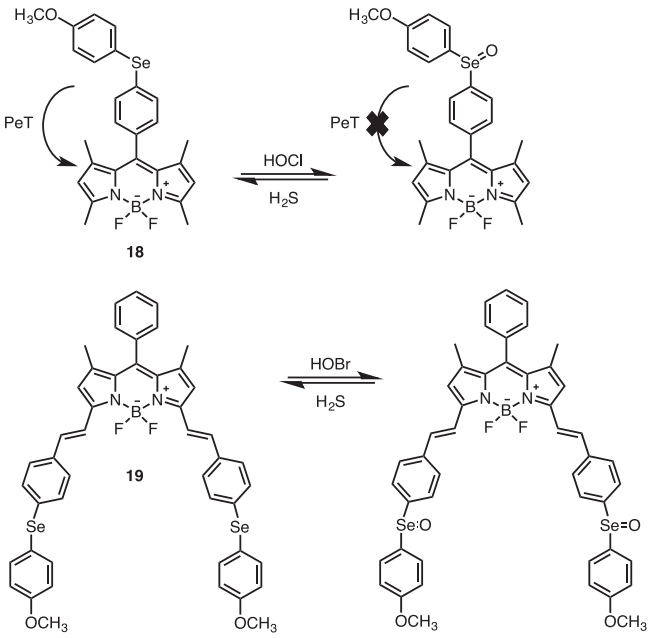

Fig. 15. Reversible probes for detection of HOCl and HOBr.

Wu and Venkatesan developed a diphenyltelluride substituted BODIPY **20** for intracellular monitoring of HOCl, which has a similar sensing mechanism with organoselenium modified probes (Fig. 16) [55]. Selective oxidation of tellurium with HOCl stops PeT and restores emission at 531 nm. Further incubation of **20** with RAW264.7 cells displays a nice turn-on response after stimulation with PMA on confocal imaging. The treatment of the cells with GSH quenches the fluorescence as a result of the reduction of tellurium. Recently, the same group reported another HOCl probe **21** carrying imine group as a selective reaction site (Fig. 16) [56]. The probe is non-fluorescent due to the (C=N) isomerization. Oxidation of the imine to an aldehyde reactivates the fluorescence, yielding 6-fold turn-on response. Confocal images clearly demonstrate the capability of **21** to monitor intracellular HOCl selectively in living cells. In another report, Wu et al. utilized a different reaction site for HOCl capture (Fig. 16) [57]. Probe **22** was modified with hydrazone moiety and it is weakly fluorescent due to the isomerization as in the case of **21**. Oxidation induced intramolecular cyclization yields a highly emissive product. The detection limit of the probe was calculated to be 2.4 nM and it was successfully used to image HOCl in RAW264.7 cells.

Emrullahoglu group utilized an aldoxime functionalized probe for selective imaging of HOCl in living cells [58]. Probe **23** is almost non-emissive as a result of C=N–OH isomerization. Oxidative dehydrogenation of aldoxime group in the presence of HOCl transforms aldoxime to a nitrile oxide and results in a rapid turn-on response (48-fold) in emission intensity at 529 nm, while causing a blue shift in absorption maximum (514 nm → 502 nm). Other potentially competing reactive oxygen species do not trigger any fluorescence enhancement, suggesting the selectivity of the probe toward HOCl. Additionally, fluorescence microscopy imaging of MCF10A cells stained with **23** shows increased intracellular fluorescence upon HOCl treatment, validating the feasibility of the probe for HOCl imaging in living cells (see Fig. 17).

Mitochondria is well known with high level of ROS generation, thus it is highly critical to track mitochondrial HOCl generation to understand its intracellular impact. Accordingly, Peng et al. designed an oxime bearing and mitochondria localizing BODIPY probe **24** for selective imaging of mitochondrial HOCl (Fig. 18) [59]. C=N isomerization favors the non-radiative decay processes

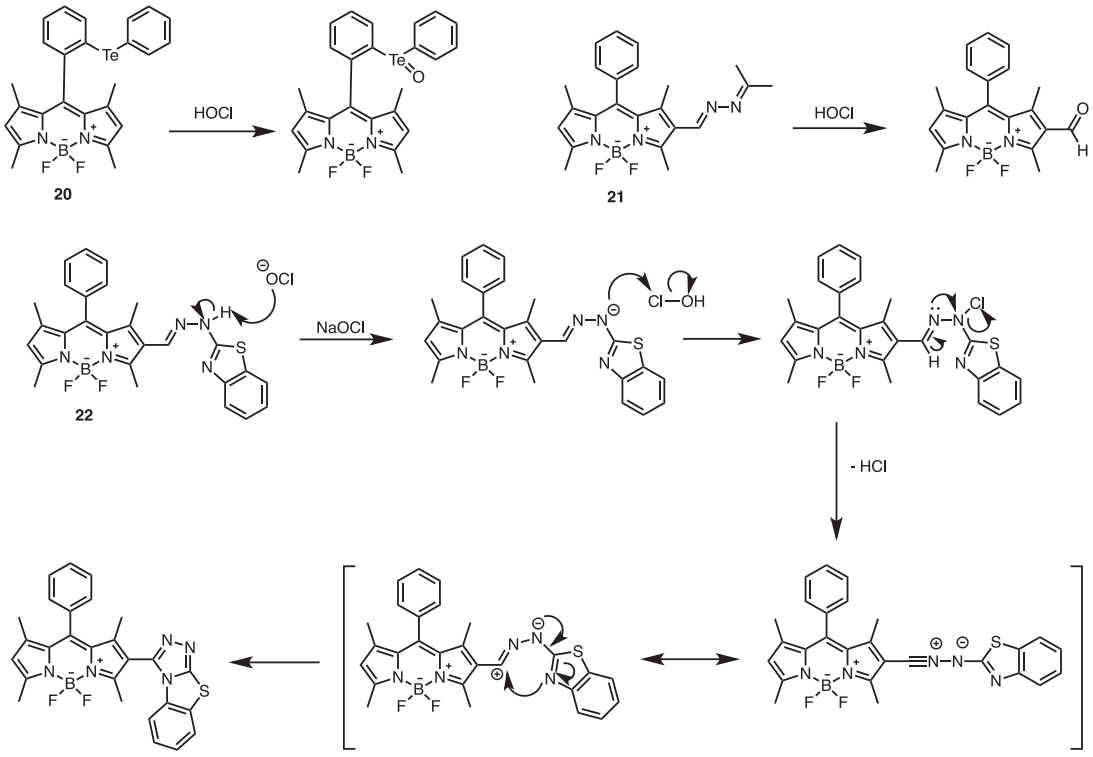

Fig. 16. Tellurium oxidation (**20**) and C=N isomerization based probes (**21** and **22**) for HOCl imaging.

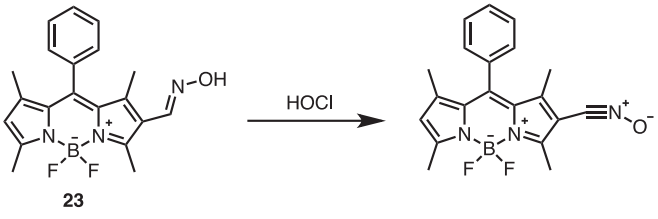

Fig. 17. HOCl-induced oxidative dehydrogenation on a BODIPY core.

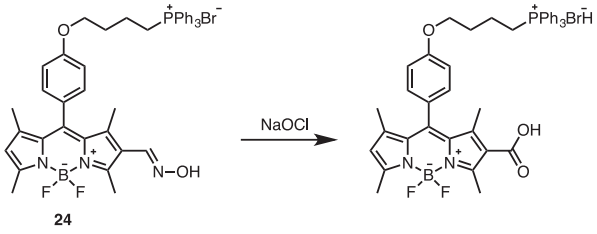

Fig. 18. A Mitochondria targeted fluorescent probe for HOCl imaging.

in the excited states and makes the probe non-emissive, while triphenylphosphonium group confers mitochondria-targeting. Oxidation of oxime to carboxylic acid increases the fluorescence intensity at 529 nm. In the case of absorption signal, a 13 nm blue shift was observed, which allows naked-eye detection of HOCl. The probe is highly selective over other ROS/RNS and confocal imaging studies show successful imaging of mitochondrial HOCl in living cells.

3.2.3. Detection of hydroxyl radical in living cells

Cosa group aimed to monitor another important ROS, the hydroxyl radical, and designed probe **25** containing α-tocopherol (similar to chromanol moiety), which was targeted to mitochondria via triphenylphosphonium substitution (Fig. 19) [60]. Chromanol has dual roles: (i) it is a PeT donor and quenches the fluorescence of BODIPY core, and (ii) it behaves as a radical scavenger. Reaction of chromanol with $ROO^{\cdot}$ blocks PeT and enhances the fluorescence emission of the probe. Imaging studies with live fibroblast cells prove the capability of the probe for intracellular monitoring of hydroxyl radical (8-fold turn-on) as well as the mitochondria targeting. Another similar probe **26**, from the same group, was used to track lipid peroxyl radicals in primary hippocampal neuronal cultures (Fig. 19) [61].

3.2.4. Detection of peroxynitrite in living cells

Peroxynitrite ($ONOO^-$) is a very short-lived RNS, which is formed by the reaction between NO and superoxide ions. Abnormal level of $ONOO^-$ is associated with several diseases, including multiple sclerosis, cancer, neurodegenerative diseases, stroke, and septic shock [43]. Consequently, the detection of intracellular

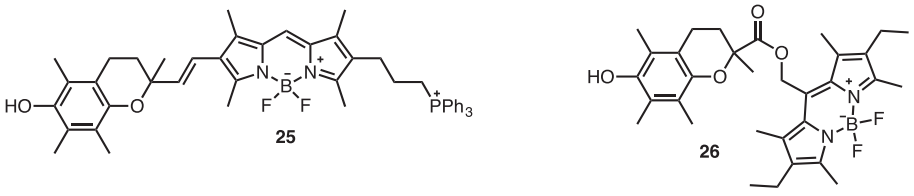

Fig. 19. Molecular structures of hydroxyl radical selective probes.

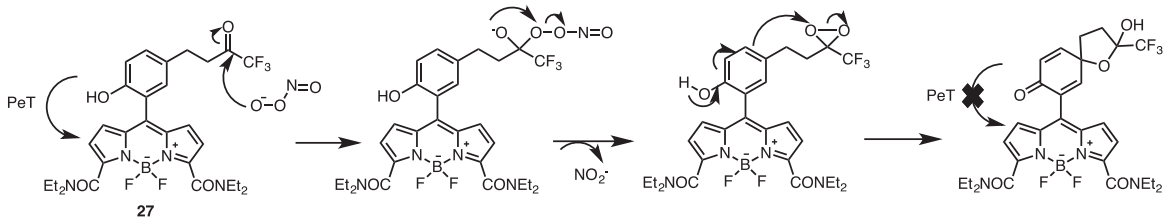

Fig. 20. A BODIPY based probe for peroxynitrite imaging in murine macrophage cells.

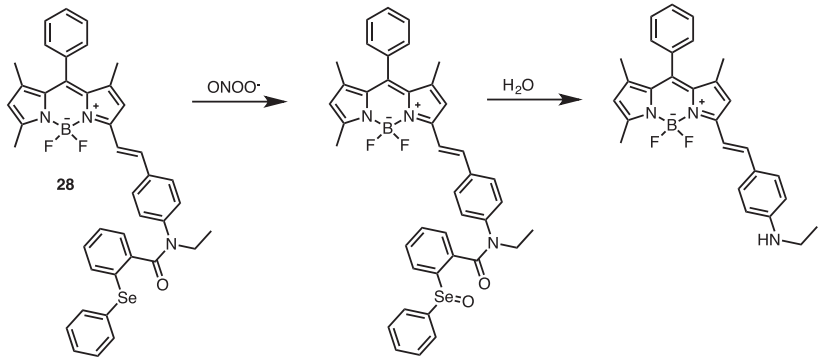

Fig. 21. Selective selenoxide spirocyclization reaction for the detection of peroxynitrite in living cells.

peroxynitrite has attracted great attention in recent years. Yang and coworkers introduced a green-emitting probe **27** for selective cellular monitoring of $ONOO^-$ (Fig. 20) [62]. The probe is weakly emissive as a result of PeT, however, reaction of ketone with peroxynitrite triggers intramolecular cyclization, which blocks the PeT and induces a great turn-on response in fluorescence at 539 nm. Testing the probe with other ROS/RNS shows great selectivity toward $ONOO^-$. Strong fluorescence was also observed on confocal microscopy of **27**-incubated murine macrophage cells upon stimulations with PMA, interferon-γ and lipopolysaccharide (LPS).

Han et al. reported another fluorescent probe based on selenoxide spirocyclization for the selective peroxynitrite detection (Fig. 21) [63]. Probe **28** has an absorption maximum at 559 nm and a strong fluorescence at 572 nm. Reaction of $ONOO^-$ with diaryl selenide first forms selenoxide, which then favors the spirodioxyselenurane formation. The modulation of the intramolecular charge transfer mechanism through a peroxynitrite specific reaction shifts the absorption maximum to 594 nm, while quenching the emission of the probe. The probe was successfully employed to detect intracellular $ONOO^-$ in RAW264.7 cells.

3.2.5. Detection of nitroxyl in living cells

Nitroxyl (HNO) holds great physiological and pathological importance. Particularly, recent studies showed that it has potential roles in treatment of heart failure [43]. Thus, it has been a significant part of current research efforts. Two near-IR emitting aza-BODIPY based probes were developed by Chen group (**29** and **30**) (Fig. 22) [64,65]. Compound **29** contains two diphenylphosphinobenzyl groups as selective reaction sites for HNO [63]. Upon HNO addition, one unit forms aza-ylide and a further intramolecular reaction gives a phenol, whereas the other diphenylphosphinobenzyl moiety yields phosphine oxide. These changes in the structure of the probe shift the absorption maximum from 672 nm to 706 nm and co increases the fluorescence intensity of the probe. **29** is highly selective toward HNO and shows remarkable turn-on responses both in *in vitro* and *in vivo* imaging studies. The second probe (**30**) of the same group utilizes the similar design principles, however, it was targeted to lysosome by modifying the aza-BODIPY core with alkylmorpholine (Fig. 22) [65]. Confocal images highlight both *in vitro* and *in vivo* detection of lysosomal HNO successfully.

3.3. Selective probes for gaseous molecules

Biologically relevant gaseous molecules namely, hydrogen sulfide (H_2S), nitric oxide (NO), and carbon monoxide (CO) are produced within the cells and play important roles in signaling mechanisms [66]. H_2S, for instance, is generated in cytosol or mitochondria from cysteine in the presence of certain enzymes. Hydrogen sulfide is a gasotransmitter and regulates numerous vital systems ranging from neuronal and cardiovascular to gastrointestinal [66]. Overexpression of H_2S is clearly associated with serious diseases such as Alzheimer's diseases, diabetes, liver indications, and Down's syndrome [66]. Nitric oxide is another significant gaseous signaling molecule, which is a free radical produced endogenously by nitric oxide synthases. Similar to H_2S, it contributes to important processes in several physiological systems such as immune, cardiovascular, and neuronal. Misregulation of NO triggers the emergence of serious problems such as cancer and neurodegenerative diseases [66]. Carbon monoxide is the third member of gasotransmitter family. CO is produced from heme with the help of heme oxygenase [67]. In combination with H_2S and NO, it takes part in highly important physiological and pathological conditions [66]. Consequently, detection and monitoring of all these three molecules in living cells are highly critical, and numerous fluorescent probes have been reported, including BODIPY based ones [66,68–70]. Since these small molecules have high reactivity, common strategy is to design chemodosimeters with selective reaction sites specific to the targeted analyte.

3.3.1. Detection of hydrogen sulfide in living cells

H_2S-mediated reduction of azide to amine is one of the widely used reactions to detect H_2S selectively. Accordingly, Talukdar and coworkers introduced an azide-modified BODIPY **31** to image intracellular H_2S (Fig. 23) [71]. The probe is non-emissive because of the PeT taking place from α-nitrogen of azido group to the

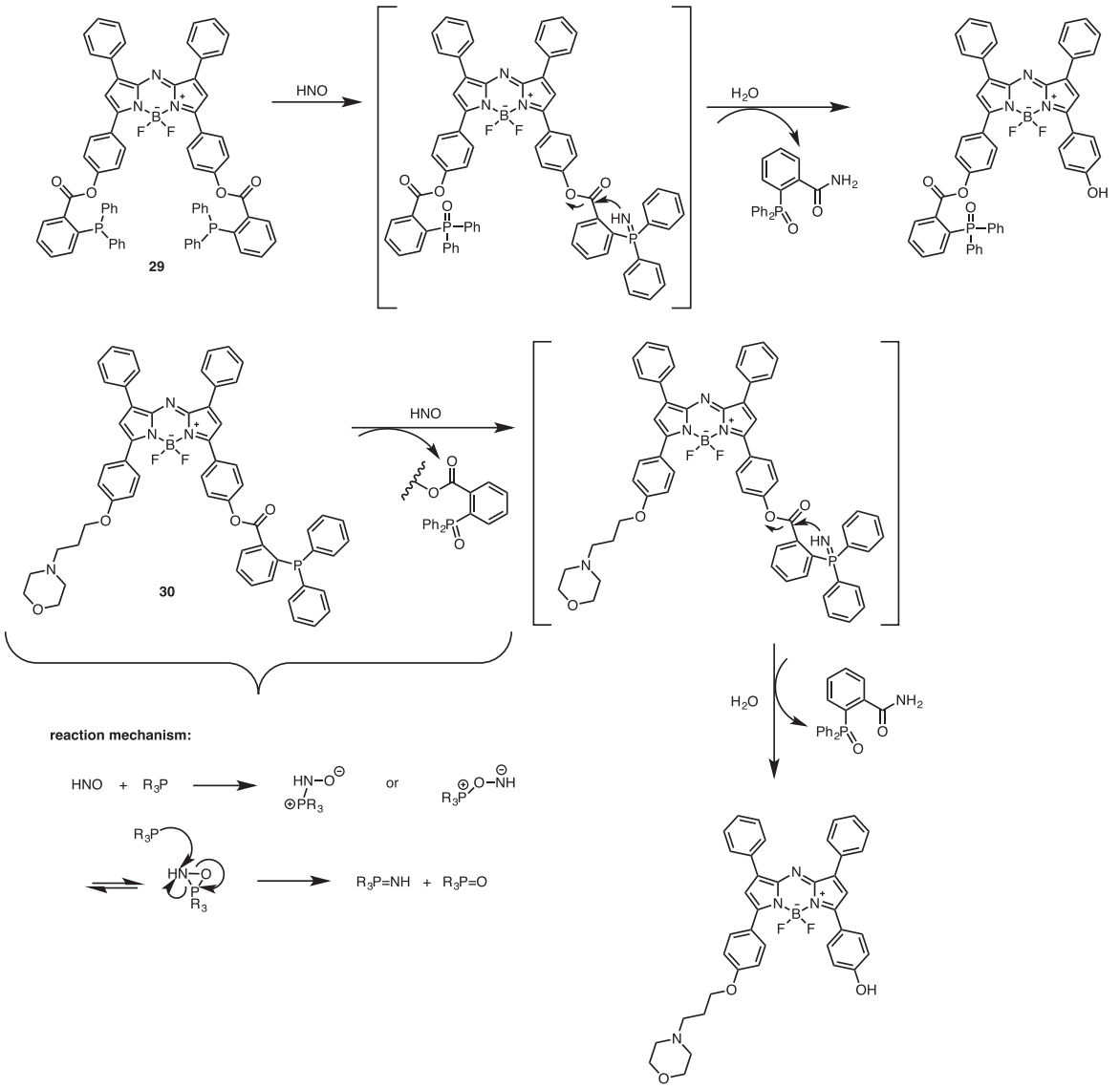

Fig. 22. Near-IR emitting aza-BODIPYs for HNO imaging.

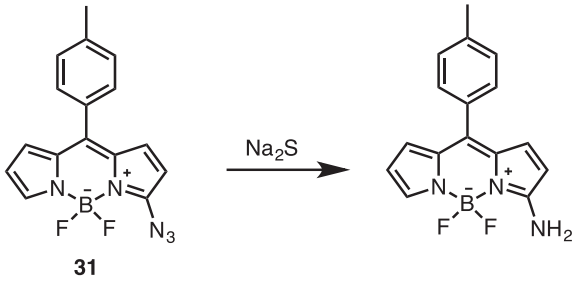

Fig. 23. Azide reduction reaction for H_2S monitoring.

BODIPY core. Selective reduction of azide to amine reactivates the fluorescence at 520 nm and displays a 28-fold turn-on response. At the same time, absorption maximum was blue-shifted upon reduction. The detection limit was calculated to be 259 nM and reaction time was found as 10 s in HEPES buffer and 30 s in serum albumin. Compound **31** was also incubated with HeLa cells, and confocal images show the expected green emission as a result of the reaction of the probe with H_2S upon Na_2S incubation.

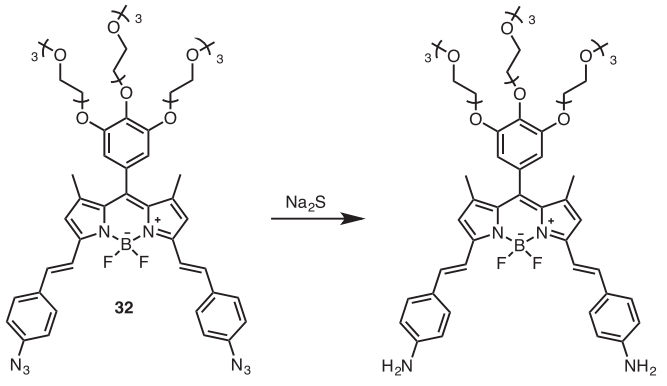

Fig. 24. A red-shifted BODIPY based probe for selective detection of H_2S in living cells.

Akkaya group also utilized the reduction of azide to amine for H_2S detection in living cells [72]. Probe **32** contains azido-appended 3,5-distyryl groups (Fig. 24). Selective reduction of azide results in a 20 nm red shift in the absorption spectrum that is

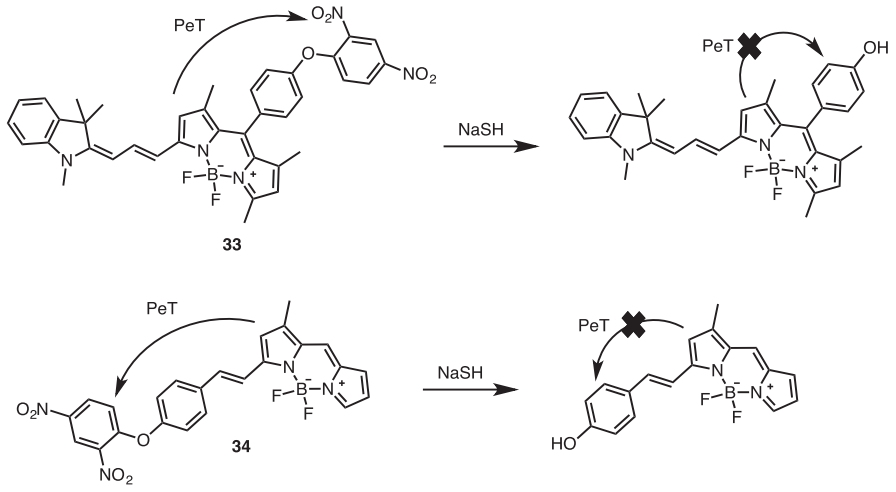

Fig. 25. Molecular structures of **32** and **33**.

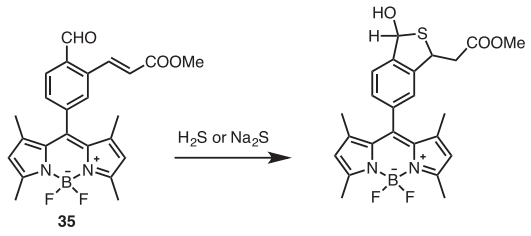

Fig. 26. A Michael addition reaction based probe **35** for H_2S detection.

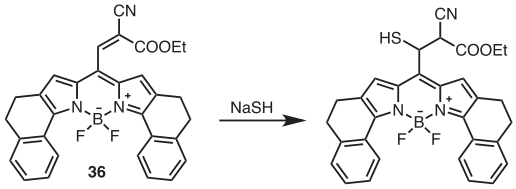

Fig. 27. H_2S monitoring in living cells with a red-shifted BODIPY based probe bearing *meso*-cyanoacetate moiety.

caused by the changes in the ICT character of the probe. At the same time, fluorescence was quenched by 85% upon H_2S addition due to the activation of PeT process. Turn-off type response was also investigated using confocal imaging; the treatment of MCF-7 cells with the probe demonstrated the applicability of **32** in live cell imaging.

Lin group made use of another reaction-based on the thiolysis of dinitrophenyl ether for fluorescent imaging of H_2S (Fig. 25) [73]. They designed and synthesized *meso*-dinitrophenyl substituted and red-shifted BODIPY based probe **33**. Selective removal of dinitrophenyl group by H_2S yields a highly emissive probe at 708 nm (18-fold turn-on). Other potentially competing biological molecules do not induce any significant fluorescence responses. Selectivity of the reaction particularly arises from different pK_a values of H_2S (6.9) and other bio-thiols (pK_a around 8.5) Fluorescence enhancement was also detected in living MCF-7 cells successfully. Recently, Li et al. reported a similar approach by applying the dinitrophenyl reactivity toward H_2S in their design **34** (Fig. 25) [74]. A turn-on response was detected at 570 nm upon titrating the probe with increasing concentrations of NaHS. Confocal images of HeLa cells that were treated with the probe demonstrated the potential of **34** to monitor intracellular H_2S.

Qian and Karpus designed a BODIPY based probe (**35**) for intracellular detection of H_2S (Fig. 26) [75]. The probe is almost non-fluorescent prior to H_2S-induced reactions. Upon the addition of Na_2S, sulfide ion is added to aldehyde group to yield a hemithioacetal. The Michael addition of the –SH group of the hemithioacetal to unsaturated acrylate ester gives a thioacetal, and increases the fluorescence intensity. Selectivity of the probe was also tested with other bio-thiols, confirming the preferential reactivity toward H_2S. Confocal images prove that these sequential reactions can also take place intracellularly in HeLa cells.

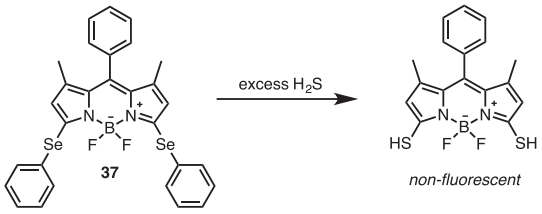

Fig. 28. Substitution reaction-triggered detection of H_2S.

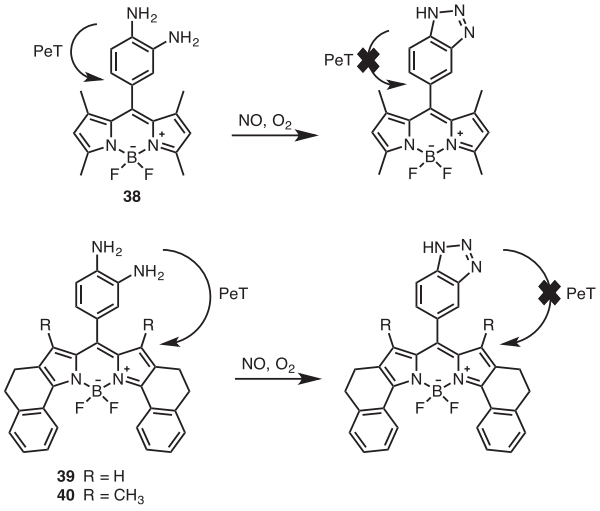

Fig. 29. Phenylenediamine substituted BODIPY based probes for selective detection of NO.

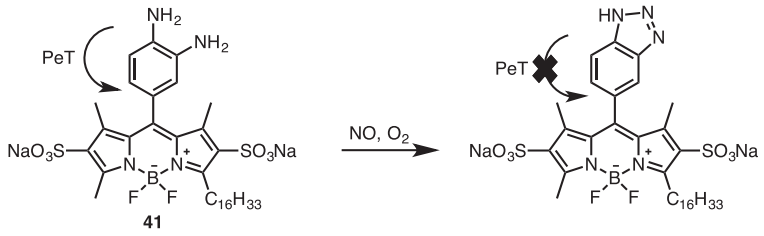

Fig. 30. Molecular structure of water-soluble NO-selective probe **41**.

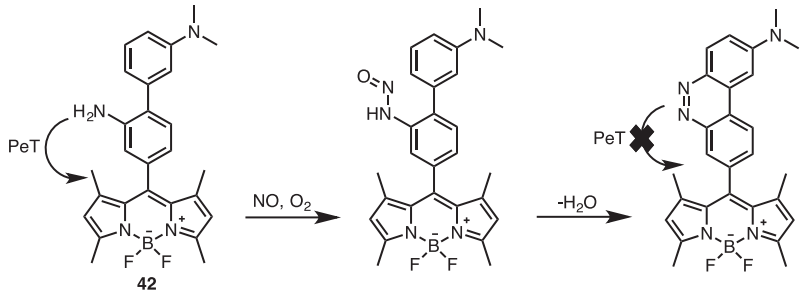

Fig. 31. Probe **42** for intracellular imaging of NO.

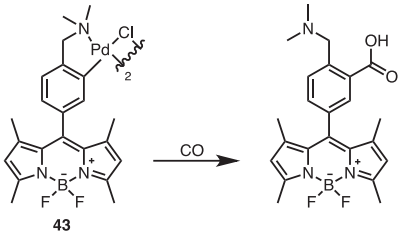

Fig. 32. A carbon monoxide selective probe **43**.

Zhao and coworkers reported a NIR-emitting probe **36** that employs a Michael addition reaction for the detection of H_2S (Fig. 27) [76]. The probe carries ethyl cyanoacetate moiety as a selective reaction site. Upon the addition of NaSH, in the sensing mechanism, Michael addition takes place and saturates the double bond, yielding a 40-fold turn-on in the emission and a blue shift in the absorption signal. Furthermore, confocal images of SMMC-7721 cells, which were incubated with the probe, possess a remarkable red emission.

Recently, Guo and Qin developed a phenylselenium substituted BODIPY (**37**) for detection of H_2S in living cells [77]. The probe is highly emissive, however, addition of excess H_2S promotes the substitution reaction between phenylselenium and sulfhydryl groups, which quenches the fluorescence intensity (Fig. 28). **37** shows a 71 nm blue-shifted absorption maximum upon H_2S reaction. The probe is highly selective toward H_2S as no significant response was observed when it was tested with other reactive species, and the detection limit was calculated to be 0.0025 μM. The probe is also compatible with live cell imaging. Confocal microscopy imaging of BHK cells displayed the expected turn-off response upon Na_2S incubation.

3.3.2. Detection of nitric oxide in living cells

Nagano group designed a NO selective BODIPY based fluorescent probe **38** in 2004 (Fig. 29) [78]. The probe displays very weak fluorescence as a result of active PeT mechanism, which is triggered by phenylenediamine moiety. Selective reaction of the PeT donor with NO forms the triazole ring that stops PeT and enhances the fluorescence intensity of the probe. Wang et al. also applied the same approach on two red-shifted BODIPY cores (**39** and **40**) (Fig. 29) [79]. Probes were suitable for intracellular NO imaging in ECv-304 cells and tissues.

Wang group also introduced an amphiphilic BODIPY based probe **41** bearing a phenylenediamine moiety to image the extracellular NO released from the living cells (Fig. 30) [80]. Hydrophilic moieties on the fluorophore core keep the NO selective reaction site (phenylenediamine) out of the cell, and long alkyl chains satisfy the cell membrane localization. The selective reaction of phenylenediamine with extracellular NO restores the fluorescence by blocking the PeT. Confocal imaging of RAW264.7 and ECV-304 cells show the capability of the probe to monitor the trafficking of NO in living cells.

Guo et al. developed a new reaction site (2-amino-3′-dimethyla minobiphenyl, AD) for selective detection of NO and attached it on to a BODIPY core **(42)** for live cell imaging (Fig. 31) [81]. Besides being a NO selective reacting moiety, AD also serves as a PeT donor, which quenches the fluorescence of the probe. Upon reacting with NO, the generated diazo product reactivates the fluorescence by blocking the PeT. Intracellular NO was successfully detected with the help of **42** in DEA-NONOate treated HL-7702 cells.

3.3.3. Detection of carbon monoxide in living cells

Chang group reported a carbon monoxide selective fluorescent probe **43** (Fig. 32) [82]. The probe is almost non-fluorescent as a result of palladium induced heavy atom electronics effects. Addition of CO releases palladium through carbonylation reaction, resulting in a highly emissive probe with a 10-fold turn-on response at 507 nm. Fluorescence response of **43** was also tested in the presence competing reactive oxygen, nitrogen, and sulfur species and fluorescence enhancement could not be observed, suggesting the selectivity of the probe toward CO. Changing intracellular CO levels was also monitored in **43** incubated HEK293T cells. It was also shown that the palladium coordination did not cause any cytotoxicity and the probe is compatible with live cell imaging.

4. Conclusion

As the palette of reactions that are specific for different analytes of particular interest become richer, there is no doubt that new and more capable probes will be developed. Bodipy dyes, as a class of remarkably versatile chromophores with tunable photophysical, chemical, and photochemical properties would naturally feature in the structures of most useful probes. We expect Bodipy probes to hold on to the center stage of probe development for many years to come.

Acknowledgement

The authors gratefully acknowledge support from Bilkent University.

References

[1] J. Chan, S.C. Dodani, C.J. Chang, Nat. Chem. 4 (2012) 973.
[2] R.Y. Tsien, Biochemistry-US 19 (1980) 2396.
[3] R.J. Lakowicz, Principles of Fluorescence Spectroscopy, Springer, New York, 1999.
[4] R.P. Haugland, Handbook of Fluorescent Probes and Research Products, Molecular Probes, 2002.
[5] A.W. Czarnik, American Chemical Society. Division of Organic Chemistry. American Chemical Society. Meeting: Fluorescent Chemosensors for Ion and Molecule Recognition, American Chemical Society, Washington, DC, 1993.
[6] C.J. Weijer, Science 300 (2003) 96.
[7] B.N.G. Giepmans, S.R. Adams, M.H. Ellisman, R.Y. Tsien, Science 312 (2006) 217.
[8] J.S. Wu, W.M. Liu, J.C. Ge, H.Y. Zhang, P.F. Wang, Chem. Soc. Rev. 40 (2011) 3483.
[9] A.W. Czarnik, Acc. Chem. Res. 27 (1994) 302.
[10] R. Martinez-Manez, F. Sancenon, Chem. Rev. 103 (2003) 4419.
[11] S.K. Kim, H.N. Kim, Z. Xiaoru, H.N. Lee, J.H. Soh, K.M.K. Swamy, J. Yoon, Supramol. Chem. 19 (2007) 221.
[12] H. Kobayashi, M. Ogawa, R. Alford, P.L. Choyke, Y. Urano, Chem. Rev. 110 (2010) 2620.
[13] Z.S. Yoon, S.B. Noh, D.-G. Cho, J.L. Sessler, D. Kim, Chem. Commun. (2007) 2378.
[14] P.D. Beer, P.A. Gale, Angew. Chem. Int. Ed. 41 (2001) 486.
[15] B. Valeur, I. Leray, Coord. Chem. Rev. 205 (2000) 3.
[16] G. Ulrich, R. Ziessel, A. Harriman, Angew. Chem. Int. Ed. 47 (2008) 1184.
[17] T. Kowada, H. Maeda, K. Kikuchi, Chem. Soc. Rev. 44 (2015) 4953.
[18] Y. Ni, J. Wu, Org. Biomol. Chem. 12 (2014) 3774.
[19] A. Loudet, K. Burgess, Chem. Rev. 107 (2007) 4891.
[20] H. Lu, J. Mack, Y. Yang, Z. Shen, Chem. Soc. Rev. 43 (2014) 4778.
[21] D.-G. Cho, J.L. Sessler, Chem. Soc. Rev. 38 (2009) 1647.
[22] M.E. Jun, B. Roy, K.H. Ahn, Chem. Commun. 47 (2011) 7583.
[23] S.H. Jung, X.Q. Chen, J.S. Kim, J. Yoon, Chem. Soc. Rev. 42 (2013) 6019.
[24] X. Chen, Y. Zhou, X.J. Peng, J. Chem. Soc. Rev. 39 (2010) 2120.
[25] S. Shahrokhian, Anal. Chem. 73 (2001) 5972.
[26] S. Seshadri, A. Beiser, J. Selhub, P.F. Jacques, I.H. Rosenberg, R.B. D'Agostino, P. W.F. Wilson, P.A. Wolf, N. Engl, J. Med. 346 (2002) 476.
[27] T.P. Dalton, H.G. Shertzer, A. Puga, Annu. Rev. Pharmacol. Toxicol. 39 (1999) 67.
[28] R.A. Cairns, I.S. Harris, T.W. Mak, Nat. Rev. Cancer 11 (2011) 85.
[29] M. Isik, T. Ozdemir, I. Simsek-Turan, S. Kolemen, E.U. Akkaya, Org. Lett. 15 (2013) 216.
[30] M. Işık, R. Guliyev, S. Kolemen, Y. Altay, B. Senturk, T. Tekinay, E.U. Akkaya, Org. Lett. 16 (2014) 3260.
[31] S. Madhu, R. Gonnade, M. Ravikanth, J. Org. Chem. 78 (2013) 5056.
[32] J. Zhang, X.-D. Jiang, X. Shao, J. Zhao, Y. Su, D. Xi, H. Yu, S. Yue, L.-J. Xiao, W. Zhao, RSC Adv. 4 (2014) 54080.
[33] L.-Y. Niu, Y.-S. Guan, Y.-Z. Chen, L.-Z. Wu, C.-H. Tung, Q.-Z. Yang, J. Am. Chem. Soc. 134 (2012) 18928.
[34] L.-Y. Niu, Q.-Q. Yang, H.-R. Zheng, Y.-Z. Chen, L.-Z. Wu, C.-H. Tung, Q.-Z. Yang, RSC Adv. 5 (2015) 3959.
[35] D.H. Ma, D. Kim, E. Seo, S.-J. Lee, K.H. Ahn, Anlayst 140 (2015) 422.
[36] J. Shao, H. Sun, H. Guo, S. Ji, J. Zhao, W. Wu, X. Yuan, C. Zhang, T.D. James, Chem. Sci. 3 (2012) 1049.
[37] D. Kand, T. Saha, M. Lahiri, P. Talukdar, Org. Biomol. Chem. 13 (2015) 8163.
[38] J. Zhang, X. Bao, J. Zhou, F. Peng, H. Ren, X. Dong, W. Zhao, Biosens. Bioelectron. 85 (2016) 164.
[39] B. Halliwell, J.M.C. Gutteridge, Free Radicals in Biology and Medicine, Oxford University Press, Oxford, 2007, pp. 1–677.
[40] B.C. Dickinson, C.J. Chang, Nat. Chem. Biol. 7 (2011) 504.
[41] C. Nathan, J. Clin. Invest. 111 (2003) 769.
[42] P.F. Bove, A. van der Vliet, Free Radical Biol. Med. 41 (2006) 515.
[43] X. Chen, F. Wang, J.Y. Hyun, T. Wei, J. Qiang, X. Ren, I. Shin, J. Yoon, Chem. Soc. Rev. 45 (2016) 2976.
[44] T. Nagano, Chem. Rev. 102 (2002) 1235.
[45] B.C. Dickinson, D. Srikun, C.J. Chang, Curr. Opin. Chem. Biol. 14 (2010) 50.
[46] X. Chen, X. Tian, I. Shin, J. Yoon, Chem. Soc. Rev. 40 (2011) 4783.
[47] S.T. Manjare, S. Kim, W.D. Heo, D.G. Churchill, Org. Lett. 16 (2014) 410.
[48] S. Bag, J.-C. Tseng, J. Rochford, Org. Biomol. Chem. 13 (2015).
[49] Z.-N. Sun, F.-Q. Liu, Y. Chen, P.K. Hang-Tam, D. Yang, Org. Lett. 10 (2008) 2171.
[50] J.J. Hu, N.-K. Wong, Q. Gu, X. Bai, S. Ye, D. Yang, Org. Lett. 16 (2014) 3544.
[51] J. Kim, Y. Kim, Analyst 139 (2014) 2986.
[52] S.-R. Liu, S.-P. Wu, Org. Lett. 15 (2013) 878.
[53] B. Wang, P. Li, F. Yu, P. Song, X. Sun, S. Yang, Z. Lou, K. Han, Chem. Commun. 49 (2013) 1014.
[54] B. Wang, P. Li, F. Yu, J. Chen, Z. Qu, K. Han, Chem. Commun. 49 (2013) 5790.
[55] P. Venkatesan, S.-P. Wu, Analyst 140 (2015) 1349.
[56] W.-C. Chen, P. Venkatesan, S.-P. Wu, New J. Chem. 39 (2015) 6892.
[57] W.-C. Chen, P. Venkatesan, S.-P. Wu, Anal. Chim. Acta 882 (2015) 68.
[58] M. Emrullahoglu, M. Üçüncü, E. Karakuş, Chem. Commun. 49 (2013) 7836.
[59] G. Cheng, J. Fan, W. Sun, K. Sui, X. Jin, J. Wang, X. Peng, Analyst 138 (2013) 6091.
[60] K. Krumova, L.E. Greene, G. Cosa, J. Am. Chem. Soc. 135 (2013) 17735.
[61] A. Khatchadourian, K. Krumova, S. Boridy, A.T. Ngo, D. Maysinger, G. Cosa, Biochemistry 48 (2009) 5658.
[62] Z.-N. Sun, H.-L. Wang, F.-Q. Liu, Y. Chen, P. Kwong, H. Tam, D. Yang, Org. Lett. 11 (2009) 1887.
[63] B. Wang, F. Yu, P. Li, X. Sun, K. Han, Dyes Pigm. 96 (2013) 383.
[64] P. Liu, X. Jing, F. Yu, C. Lv, L. Chen, Analyst 140 (2015) 4576.
[65] X. Jing, F. Yu, L. Chen, Chem. Commun. 50 (2014) 14253.
[66] X. Zhou, S. Lee, Z. Xu, J. Yoon, Chem. Rev. 115 (2015) 7944.
[67] S.W. Ryter, J. Alam, A.M.K. Choi, Physiol. Rev. 86 (2006) 583.
[68] R.A. Potyrailo, C. Surman, N. Nagraj, A. Burns, Chem. Rev. 111 (2011) 7315.
[69] K. Arshak, E. Moore, G.M. Lyons, J. Harris, S. Clifford, Sensor Rev. 24 (2004) 181.
[70] O.S. Wenger, Chem. Rev. 113 (2013) 3686.
[71] T. Saha, D. Kand, P. Talukdar, Org. Biomol. Chem. 11 (2013) 8166.
[72] T. Ozdemir, F. Sozmen, S. Mamur, T. Tekinay, E.U. Akkaya, Chem. Commun. 50 (2014) 5455.
[73] X. Cao, W. Lin, K. Zheng, L. He, Chem. Commun. 48 (2012) 10529.
[74] J. Cheng, B. Shao, S. Zhang, Y. Hu, X. Li, RSC Adv. 5 (2015) 65203.
[75] Y. Qian, J. Karpus, O. Kabil, S.-Y. Zhang, H.-L. Zhu, R. Banerjee, J. Zhao, C. He, Nat. Commun. 2 (2011) 495.
[76] J. Zhang, J. Zhou, X. Dong, X. Zheng, W. Zhao, RSC Adv. 6 (2016) 51304.
[77] D. Gong, X. Zhu, Y. Tian, S.-C. Han, M. Deng, A. Iqbal, W. Liu, W. Qin, H. Guo, Anal. Chem. 89 (2017) 1801.
[78] Y. Gabe, Y. Urano, K. Kikuchi, H. Kojima, T. Nagano, J. Am. Chem. Soc. 126 (2004) 3357.
[79] Zhang, J.-B. Chen, X.-F. Guo, H. Wang, H.-S. Zhang, Anal. Chem. 86 (2014) 3115.
[80] H.-W. Yao, X.-Y. Zhu, X.-F. Guo, H. Wang, Anal. Chem. 88 (2016) 9014.
[81] X. Lv, Y. Wang, S. Zhang, Y. Liu, J. Zhang, W. Guo, Chem. Commun. 50 (2014) 7499.
[82] B.W. Michel, A.R. Lippert, C.J. Chang, J. Am. Chem. Soc. 134 (2012) 15668.